Routing Performance Analysis of Human-Driven Delay Tolerant Networks using the Truncated Levy Walk Model [*]

Seongik Hong
Dept. of Computer Science
NC State University
shong@ncsu.edu

Injong Rhee
Dept. of Computer Science
NC State University
rhee@ncsu.edu

Seong Joon Kim
Dept. of Computer Science
NC State University
sjkim2@ncsu.edu

Kyunghan Lee
School of EECS, KAIST
kama@netsys.kaist.ac.kr

Song Chong
School of EECS, KAIST
song@ee.kaist.ac.kr

ABSTRACT

The routing performance of delay tolerant networks (DTN) is highly correlated with the distribution of inter-contact times (ICT), the time period between two successive contacts of the same two mobile nodes. As humans are often carriers of mobile communication devices, studying the patterns of human mobility is an essential tool to understand the performance of DTN protocols. From measurement studies of human contact behaviors, we find that their distributions closely resemble a form of power-law distributions called truncated Pareto. Human walk traces has a dichotomy distribution pattern of ICT; it has a power-law tendency up to some time, and decays exponentially after that time. Truncated Pareto distributions offer a simple yet cohesive mathematical model to express this dichotomy in the measured data. Using the residual and relaxation time theory [17] [4], we apply truncated Pareto distributions to quantify the performance of opportunistic routing in DTN. We further show that Truncated Levy walk (TLW) mobility model [22] commonly used in biology to describe the foraging patterns of animals [25], provide the same truncated power-law ICT distributions as observed from the empirical data, especially when mobility is confined within a finite area. This result confirms our recent finding that human walks contain similar statistical characteristics as Levy walks [22].

Categories and Subject Descriptors

C.2.1 [**Network Architecture and Design**]: Wireless Communication

General Terms

Measurement, Performance

Keywords

Mobility model, delay tolerant networks, inter-contact time, routing performance

[*]This work is supported in part by NSF NeTs 0626850, and also gift from Boeing, Phantom works.

MobilityModels'08, May 26, 2008, Hong Kong SAR, China.

1. INTRODUCTION

DTN provides a challenging environment in which communications between nodes are intermittent [9]. DTN does not assume that there exists connectivity between nodes at a certain point in time. When the nodes are disconnected, the packets are stored and forwarded through intermittent contacts established by the mobility of the nodes. In this type of networks, ICT is a key determinant of routing performance.

Many simulation and theoretical studies of DTN routing (e.g. [10] [24]) have long assumed that the ICT distribution (ICTD) of human walks follows an exponential distribution. Exponential distributions make mobility analysis tractable and the simulation results with popular mobility models [6] such as Random WayPoint (RWP) or Random Direction (RD) models can easily produce exponentially decaying ICT distributions. But recently, empirical studies [7] show that this assumption is wrong especially in the context of human mobility: the ICTD of human walks contains a power law tendency. Under the assumption that the ICTD has a power law tail, the DTN routing delays approach infinite because of the presence of infinitely long inter-contact times.

Recently, [15] shows that for random walks with home coming tendency, there exists a *characteristic time* until which the ICTD has a power law tendency and after which it decays exponentially. Concurrently, [5] also shows that mobility within a finite area is also a cause of the exponential decay of the ICTD for random walks. These finding on the exponential ICTD tails imply that the delay of opportunistic routing algorithms should be finite in contrast to the infinite delay under the power law ICTD assumption.

We do not yet have mathematical models to describe the dichotomy of ICTD that are easy enough like exponential distributions for the performance analysis of DTN routing. To solve this problem, we analyze three empirical data sets of human ICT. We observe from Maximum Likelihood Estimation (MLE) and Akaike test [16] results that the ICTD

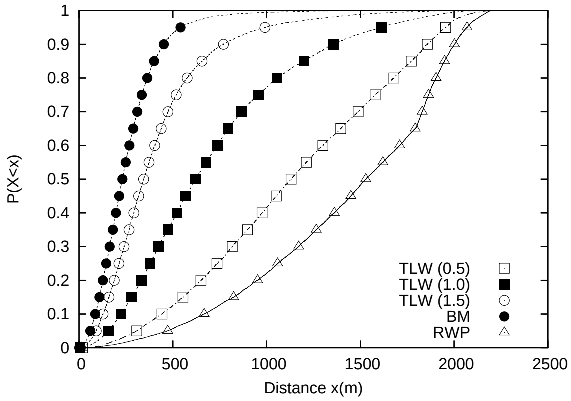

Figure 1: The CDF of user displacements from its initial position in a fixed travel time. RWP is most diffusive while BM is least diffusive. The diffusion rates of TLW are in-between. The values in the parentheses represent the Levy exponent for flight length.

closely follows a truncated Pareto distribution. Truncated Pareto distributions have a truncation point that corresponds to the characteristic time in the ICTD. We show that the closed form expression of DTN routing delay can be induced from the ICTD model.

We further show that TLW provides the same truncated Pareto ICT distributions as observed from the empirical data, especially when mobility is confined within a finite area. This result confirms our recent finding that human walks contain similar statistical characteristics as Levy walks [22].

The message delivery ratio is another important aspect of the routing performance. We first quantify the characteristic time using the relaxation time of TLW in a confined region, and show how to predict the delivery ratio using the characteristic time.

The remainder of this paper is organized as follows. In section 2, we introduce mobility models including TLW. Our experimental results on the ICTD of human walks are presented in section 3. In section 4, we study the impact of the truncated Pareto ICTD and the relaxation time on the actual performance of DTN routing algorithms in detail. In addition to the single relay case, we generalize our work to multiple relay cases.

2. TRUNCATED LEVY WALKS

A variety of mobility models have been proposed including RWP, RD, Brownian Motion (BM). These models vary in their movement characteristics. In RWP, a user chooses a random destination (waypoint) in a simulation area and a speed from a uniform distribution, respectively. In each waypoint, the user pauses for a certain period of time, and continue the process. In RD, a user chooses a random direction in which to travel, then travels to the border of the simulation area in that direction. Once the simulation boundary is reached, the user pauses for a specified time, and continues the process.

Recently, the TLW mobility model has been proposed [22]. In TLW, each flight length and pause time follow truncated power laws. During a pause, a walker stays at the location where the current flight ends. The main difference of TLW from the others is that we can easily control the level of diffusivity using its power law exponent. It makes TLW a very useful tool to describe a variety of diffusive natures of human mobility. Diffusivity plays an important role in determining the ICTD [22]. Diffusivity can be defined to be the variance of the displacement between the current position at time t and a previous position at time t_0. Fig.1 shows the amount of displacement for various mobility models plotted in Cumulative Distribution Function (CDF) forms. In this simulation, nodes are moving with same velocity and same pause time distribution in the same area. So we can consider that the difference of displacement patterns comes from the difference of their flight length distribution. The diffusivity is highly related to the amount of displacement. For example, in Fig.1 we can see that RWP is most diffusive while BM is least diffusive, and TLW is in-between.

Table 1: Notation for Levy distribution

α	exponent for flight length
β	exponent for pause time
c	scale factor
δ	skewness parameter
m	peak position
$1/\eta$	truncation point

To describe the characteristic function of TLW, let's first examine a Levy distribution with no truncation. Consider a mobility model with power law flight length distribution $p(t)$, and power law pause time distribution $\psi(t)$. Their asymptotic behavior can be represented as follows [14].

$$p(t) \sim |t|^{-(1+\alpha)} \tag{1}$$

$$\psi(t) \sim t^{-(1+\beta)}, \text{where t} > 0 \tag{2}$$

α and β have a value between 0 and 2. The special case $\alpha = 2$ (or $\beta = 2$) gives a Gaussian distribution for flight length (or pause time). A characteristic function for a stable Levy distribution in Eq.(1) is defined as follows [14].

$$L(z) = \exp\{-c|z|^{\alpha}[1 + i\delta \text{sgn}(t) \tan(\frac{\pi\alpha}{2})] + imz\} \tag{3}$$

c is a scale factor characterizing the width of the distribution; m gives the peak position; δ is a skewness parameter characterizing the asymmetry of the distribution ($\delta = 0$ gives a symmetric distribution); and $sgn(t)$ is a sign function of t. In this paper, we consider only symmetric distributions. Also we assume the maximum at $t = 0$, leading to $m = 0$, then the simplified version of Eq.(3) becomes

$$L_s(z) = \exp\{-c|z|^{\alpha}\}. \tag{4}$$

The idea of truncating a Levy distribution at some typical scale $1/\eta$ was mainly born from the analysis of financial data [23]. Its characteristic function is defined as follows.

$$T(z) = \exp\{-c\frac{(\eta^2 + z^2)^{\alpha/2}\cos(\alpha \arctan\frac{|z|}{\eta}) - \eta^{\alpha}}{\cos(\frac{\pi\alpha}{2})}\} \tag{5}$$

When $\eta \to 0$, Eq.(5) can be rewritten as

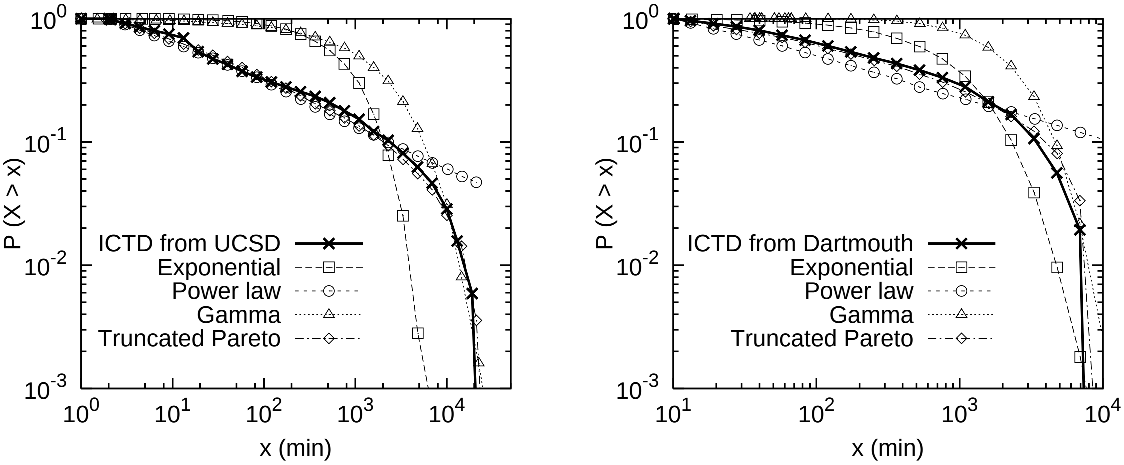

(a) UCSD (b) Dartmouth

Figure 2: The CCDF of ICT collected from UCSD and Dartmouth. Various known distributions are fitted to the measured data distribution using MLE.

$$T_s(z) \rightarrow \exp\{-c|z|^{\alpha}\} \tag{6}$$

which has the same form as Eq.(4). Eqs.(4) and (6) imply that we can consider that TLW has flight length and pause time distributions that follow Levy distributions as long as the truncation points are large enough.

Stationarity is another issue for mobility models [3]. It is known that TLW has its stationary regime and it is uniform since it has finite pause time and trip durations [22]. TLW belongs to the *random trip* class of model in [3] since its moving trajectory shows the same pattern as *Random Walk on Torus* model in wrap around boundary condition and *Billiards* in reflecting boundary condition. In this paper, we assume that all the nodes are in their stationary regime from the initial state.

3. INTER CONTACT TIMES

In this section, we show that the dichotomy of ICTD can be modeled by a truncated Pareto distribution and we can quantify the characteristic time using the relaxation time theory [2].

3.1 ICTD Fitting

We analyze three empirical data sets of human ICTs. Those data sets are traces taken in UCSD [19], Dartmouth University [11] and Infocom 2005 [12]. The UCSD data records mobility patterns of 275 wireless PDA users within a campus WiFi network for the duration of 11 weeks. The Dartmouth data contains thousands of laptop/PDA users using campus WiFi networks over years. The experiment in Infocom 2005 has inter-contact information of 41 iMotes (Bluetooth devices) carried by attendees of the conference for 3 to 4 days. We pre-process all the data except Dartmouth for which we preprocess one-month worth of contact information.

We apply *Maximum Likelihood Estimation* (MLE) [16] to fit to the complementary cumulative density function (CCDF) of the produced ICTDs from the traces, five well-known distributions: exponential, power law, gamma, Weibull and truncated Pareto distributions. The gamma and Weibull distributions are considered good candidates to describe the dichotomy patterns. Since they have heavy tail distributions with exponential decay in the end. The truncated Pareto distribution also has a power law tendency at the head part and decays exponentially at the tail. MLE is performed over the x-axis range between two minutes up to the 99% quantile of each data set. Figs. 2 and 3(a) show the CCDF of the ICTDs from each data set and the best MLE fittings for every distribution. Although the MLE itself does not give quantitative information on the closest matching distribution, we can observe visually the truncated Pareto distribution fits the best. (In Fig.2, Weibull fittings are not shown since MLE for Weibull fails in the optimization process for UCSD and Dartmouth data.)

To quantify the degree of the best fitting, we perform the *Akaike* test [8] [16]. The Akaike test gives an estimate of the expected, relative distance between the fitted distribution and the unknown true distribution obtained from the observed data. In this test, the best fitting distribution is the one giving the minimum *Akaike's Information Criteria* (AIC) value or *Akaike Weight* (AW) closest 1. The AIC and AW values for the three data sets are shown in Tables 2, 3 and 4. They find the truncated Pareto distribution to be the best fitting distribution. For other data sets that we didn't perform MLE and Akaike test, we can easily see that their ICTDs resemble truncated Pareto distribution (e.g. [7] [18]).

We also find that TLW can easily generate truncated Pareto ICT distributions. Fig.3(b) shows the simulation results using TLW. The simulation simulates 600 hours of human walks of 50 persons generated by TLW in a 3.5 by 3.5 km^2 square area with reflecting boundaries. With this boundary, if a person hits the boundary of the square, he is reflected at the boundary. The contact information is checked every 1 minute. In the simulation, the initial position of every person has a uniform distribution which is the stationary distribution of the model. We discard the first 100 hours of simulation results to avoid any transient effects. The speed of every user is set to 1 m/s for simplicity. Transmission range of mobile devices is set to 250m, which is the typi-

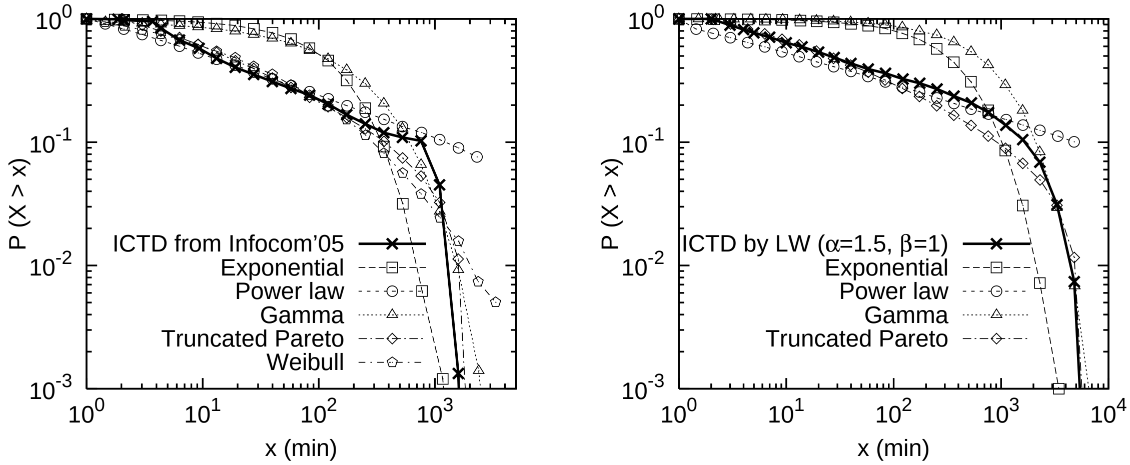

(a) Infocom 2005 (b) TLW

Figure 3: The CCDF of ICT collected from Infocom 2005 and simulation result by TLW. Various known distributions are fitted using MLE. TLW recreates the ICTD seen in the empirical data sets.

Table 2: The AIC and AW values for the ICT data from UCSD.

Distribution	AIC	AW
Exponential	3,876,400	0
Power law	3,019,400	0
Gamma	3,072,202	0
Truncated Pareto	2,976,700	1
Weibull	N/A	0

Table 3: The AIC and AW values for the ICT data from Dartmouth.

Distribution	AIC	AW
Exponential	152,730,000	0
Power law	148,270,000	0
Gamma	146,580,000	0
Truncated Pareto	143,170,000	1
Weibull	N/A	0

cal value of WiFi. The scale factors of flight lengths and pause times are set to 10 and 1, respectively. Maximum flight length and pause time are set to 3 km and 28 hours. Most of the parameters used in this paper are from [22]. Akaike test shows AW=1 for the truncated Pareto distribution, which confirms that TLW generates the same ICTD as observed from empirical data.

3.2 Characteristic Time

It has been shown that the ICTD for the RWP and RD model has exponential tail [13] [5]. Their proof uses that the node movements form a *renewal process*. For example, in RWP, the longest time duration for two nodes to finish two jumps can be interpreted as a *renewal interval*, say ζ. Since in RWP a node chooses a random destination in a simulation area so the locations of two nodes at t_0 are independent of their locations at $t_0 - \zeta$.

Now consider a similar renewal process for TLW. In the stationary regime, the locations of each node are independent of the locations at the initial time. Therefore, the renewal interval ζ is the duration for the locations of nodes to reach the stationary state from the initial state. Since the stationary state can be defined on a finite area, we can say that the equilibrium state is reached by the effect of boundaries. It means that before ζ has past, the effect of boundary will not be apparent [21]. From the fact that in infinite area without a boundary, the ICTD for any random walk model follows a power law [5], we can conjecture that the power law ICTD appears before ζ has past. This formulation explains the dichotomy of the ICTD and it can be applied to any mobility model that has its stationary regime.

Table 4: The AIC and AW values for the ICT data from Infocom 2005.

Distribution	AIC	AW
Exponential	297,340	0
Power law	262,410	0
Gamma	258,960	0
Truncated Pareto	245,890	1
Weibull	253,800	0

The relaxation time is the time elapsed until that the initial distribution of node locations reach the equilibrium state. From the above discussion, we can see that the relaxation time corresponds to the characteristic time.

For the mathematical representation of the characteristic time by TLW, we make some modifications to the approach to calculate the relaxation time in a confined area shown in [4]. We estimate the time to reach equilibrium for a 2-D TLW in a square with the size of L^2. A single step radial distribution of TLW can be approximated by the truncated version of Eq.(1). By Bachelier's equation [14](chap 3), the location after the N^{th} flight is the convolution of each transition probability. As convolution in the time domain corresponds to the multiplication in the frequency domain, from Eq.(6) we can get a new characteristic function,

$$T_s(z)^N = exp\{-cN|z|^{\alpha}\}. \tag{7}$$

Table 5: Additional notation for Section 3

ζ	typical time to reach stationarity
L	length of a side for a square area
N_m	m-th mode number
δt_f	average time duration of a single flight
δt_p	average time duration of a single pause
f_{min}	minimum length of a flight
f_{max}	maximum length of a flight
p_{min}	minimum duration of a pause
p_{max}	maximum duration of a pause

The number of flights, N, can be represented by $t/\delta t_f$ assuming zero pause time where δt_f denotes the typical time duration of a single flight. Then the relaxation time is provided by the N_m-th mode.

$$k_{N_m} = \frac{2\pi}{L} N_m \tag{8}$$

Insert Eq.(8) into Eq.(7) with $N = t/\delta t_f$ to obtain

$$T_s(z)^N = exp\{-\frac{t}{\frac{\delta t_f}{c(\frac{2\pi N_m}{L})^\alpha}}\}. \tag{9}$$

By the definition of relaxation time, after $\zeta\prime$ in Eq.(10), the distribution reaches the stationary state.

$$\zeta\prime = \frac{\delta t_f}{c(\frac{2\pi N_m}{L})^\alpha} \tag{10}$$

If we consider non-zero pause time, Eq.(10) becomes

$$\zeta = \zeta\prime + \lfloor \frac{\zeta\prime}{\delta t_f} \rfloor \delta t_p. \tag{11}$$

δt_p denotes the typical time duration of a single pause. δt_f and δt_p can be computed from the PDF of truncated Pareto distributions as shown in Eqs.(12) and (13). f_{min} and f_{max} represent the minimum and maximum flight length and p_{min} and p_{max} represent the minimum and maximum pause time.

$$\delta t_f = \begin{cases} \dfrac{\ln f_{max} - \ln f_{min}}{f_{min}^{-1} - f_{max}^{-1}} & \text{if } \alpha = 1 \\ \dfrac{\alpha}{\alpha - 1} \dfrac{f_{min}^{1-\alpha} - f_{max}^{1-\alpha}}{f_{min}^{-\alpha} - f_{max}^{-\alpha}} & \text{else} \end{cases} \tag{12}$$

$$\delta t_p = \begin{cases} \dfrac{\ln p_{max} - \ln p_{min}}{p_{min}^{-1} - p_{max}^{-1}} & \text{if } \beta = 1 \\ \dfrac{\beta}{\beta - 1} \dfrac{x_{min}^{1-\beta} - x_{max}^{1-\beta}}{x_{min}^{-\beta} - x_{max}^{-\beta}} & \text{else} \end{cases} \tag{13}$$

Finally, we need to get the best mode number (N_m) in Eq.(8) since Eq.(11) with the first mode which is generally used, gives too rough value. Fig.4 shows that the results using $N_m = 5$ are consistent with the corresponding simulation results. The simulation setup is the same as in Fig.3(b).

Fig.4 shows that the characteristic time is inversely proportional to the diffusivity of the underlying mobility model. The diffusivity of various mobility models is shown in Fig.1.

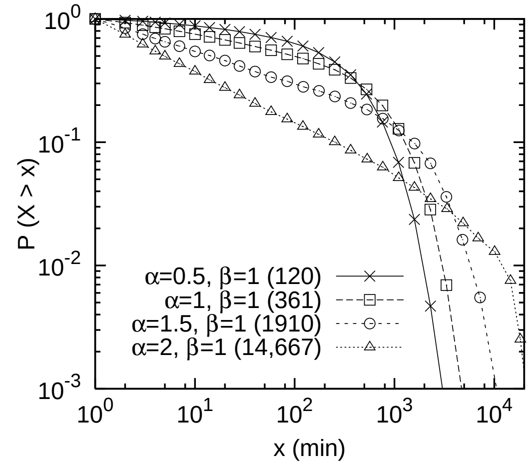

Figure 4: The ICTD of TLW. The numbers in parenthesis represent the characteristic time from analysis.

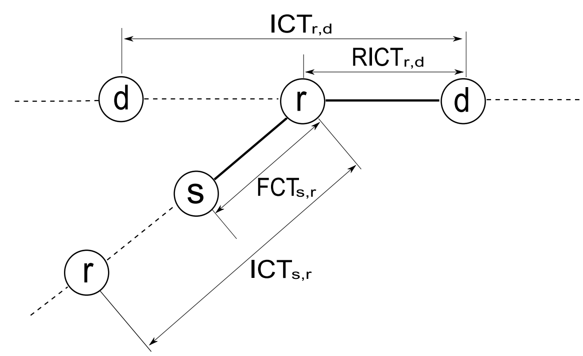

Figure 5: A DTN routing delay according to the two hop relay algorithm. FCT and RICT can be considered as the residual times of ICT.

4. ROUTING PERFORMANCE

4.1 Routing Delay

One of the most widely studied routing algorithms in DTN is two-hop relay routing [10] where a source node sends a message to the first node it contacts and then that first node acts as a relay and delivers the message when it contacts the destination node of the message. Here the period between the time that the message has originated and the time that the message is delivered to the relay node is called the first contact time (FCT) to a relay and the period after that to the time the message is delivered to the destination is called the remaining inter-contact time (RICT) between the relay and destination. In a dense network, FCT is typically negligible and RICT dominates the message delay.

The relationship between ICT and RICT in two-hop relay algorithm can be represented by the relationship between the *recurrence time* and *residual time* as shown in Fig.5. The recurrence time is the time duration between two successively recurrent events, and the residual time is the time until the next event happens from an arbitrary point in time. Let T and R denote the recurrence and residual time process, respectively. Then it is known that the following properties hold [17].

$$P(R > y) = \frac{E(T) - \int_0^y P(T > x)dx}{E(T)} \tag{14}$$

$$f_R(y) = \frac{P(T > y)}{E(T)} \tag{15}$$

In the stationary regime, we can assume enough time has past so that all the nodes have met each other at least once before a message transfer starts. Since FCT is negligible in a dense network, the routing delay of a message is approximately equal to RICT between the relay and destination nodes. Let X, Y and Z denote ICT, RICT and routing delay, respectively. In case that X follows a truncated Pareto distribution with coefficient γ between 0 and 2, the CCDF and expectation of X can be represented as follows [1].

$$\begin{aligned} P(X > x) &= \frac{x_{min}(x^{-\gamma} - x_{max}^{-\gamma})}{1 - (x_{min}/x_{max})^{\gamma}} \\ &= \frac{(x^{-\gamma} - x_{max}^{-\gamma})}{1 - x_{max}^{-\gamma}} \end{aligned} \tag{16}$$

Here, x_{min} and x_{max} denote the minimum and maximum ICTs, respectively. For simplicity, we will assume $x_{min} = 1$ in this section simplifying the above equations in Eqs.(16) and (17). Eq.(17) is a simplified form of Eq.(12).

$$E(X) = \begin{cases} \dfrac{\ln x_{max}}{1 - x_{max}^{-1}} \text{ , if } \gamma = 1 \\ \\ \dfrac{\gamma}{\gamma - 1} \dfrac{1 - x_{max}^{1-\gamma}}{1 - x_{max}^{-\gamma}} \text{ , else} \end{cases} \tag{17}$$

From Eqs.(14), (16) and (17), we get a closed form of routing delay distributions for the two hop relay protocol with a single relay as follows.

$$\begin{aligned} P(Z > t) &\simeq P(Y > t) \\ &= \frac{E(X) - \int_1^t P(X > x)dx}{E(X)} \\ &= \frac{E(X) - \frac{(t-1)(1-\gamma) - x_{max}^{\gamma}(t^{1-\gamma} - 1)}{(\gamma-1)(x_{max}^{\gamma} - 1)}}{E(X)} \\ &= \frac{g(\gamma) + x_{max}^{\gamma}(t^{1-\gamma} - 1) - (t-1)(1-\gamma)}{g(\gamma)} \\ &= h(\gamma, x_{max}) \end{aligned} \tag{18}$$

$g(\gamma)$ denotes $\gamma(x_{max}^{\gamma} - x_{max})$. Eq.(18) shows that the routing delay is a function of γ and x_{max}. From Eq.(15), we know the PDF of the RICT, so we can get a closed form expression of the expectation for Z using Eqs.(16) and (17).

$$\begin{aligned} E(Z) &\simeq E(Y) \\ &= \int_0^{x_{max}} y \frac{P(X > y)}{E(X)} dy \\ &= \frac{1}{E(X)(1 - x_{max}^{-\gamma})} [\frac{x_{max}^{2-\gamma} - 1}{2 - \gamma} - \frac{x_{max}^{-\gamma}(x_{max}^2 - 1)}{2}] \end{aligned} \tag{19}$$

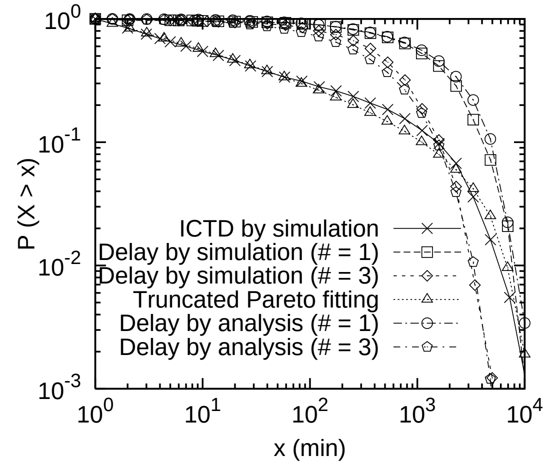

Figure 6: The ICT and DTN delay distributions with single and multiple relays. Results from both analysis and simulation are matching well. The values in parenthesis represent the number of relays.

Numerical evaluation from Eqs.(17) and (19) shows that the expectation of Z is almost ten times bigger than that of X. It is consistent with *inspection paradox* [20] [7] because Y is dominated by the large samples of X. Note that Eq.(19) implies that the expectation is always finite in contrast to the results of infinite delays under the power law ICTD [7].

In a generalized relaying algorithm [7], the source distributes the message to the first m relays that it contacts. The routing delay is the time till any copy of the message is delivered to the destination. In this case Z can be represented by $min(Y_1, \cdots, Y_m)$ where Y_i represents the RICT by the i^{th} relay. Using simple probabilistic manipulation, we can see that the CCDF of Z is a multiplication of CCDFs of Y_1 through Y_m. Then the closed form of the CCDF of Z can be shown as below.

$$\begin{aligned} P(Z > t) &= P(Y_1 > t) \cdots P(Y_m > t) \\ &= h_1(\gamma, x_{max}) \cdots h_m(\gamma, x_{max}) \\ &= h(\gamma, x_{max})^m \end{aligned} \tag{20}$$

$h_i(\gamma, x_{max})$ represents the result of Eq.(18) by the i^{th} relay.

Fig. 6 shows the results of above analysis and corresponding simulation. We can see the analysis results are consistent with the simulation results by TLW. The simulation setups are the same as used in Fig.4.

So far, we have assumed that FCTs are negligible. We now consider a case that this assumption is not valid. We need to compute FCT and add it to RICT to get the exact delay. FCT can be considered as the minimum RICT from the source node to the other nodes. Let W represent FCT. Then $W = min(Y_1, \cdots, Y_{N-1})$ where N is the total number of nodes.

$$\begin{aligned} P(W > t) &= P(Y_1 > t) \cdots P(Y_{N-1} > t) \\ &= h_1(\gamma, x_{max}) \cdots h_{N-1}(\gamma, x_{max}) \\ &= h(\gamma, x_{max})^{N-1} \end{aligned} \tag{21}$$

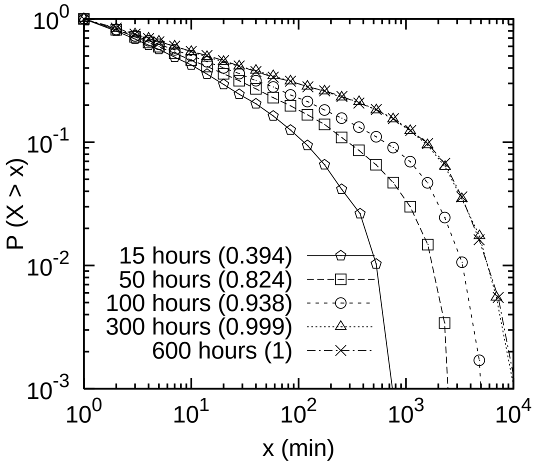

Figure 7: The ICTDs of TLW (α=1.5, β=1) according to various amount of simulated hours. The values in parenthesis represent delivery ratio. When the truncation of the ICTD comes from the insufficient duration of simulation, the delivery ratio is below one.

We covered the cases that X follows a truncated Pareto distribution, but this formulation can also be used for any distribution of X such as exponential distributions with RWP. To get the closed form of routing delays for RWP, we only need to replace Eqs.(16) and (17) with the corresponding values from exponential distributions.

4.2 Message Delivery Ratio

In this section, we study the impact of insufficient duration of measurement (or simulation) to the delivery ratio of messages. We already know that the power law ICTD experiences an exponential decay due to the effect of the boundaries, home coming tendency or the renewal interval formed by the stationarity of node locations. But another reason of the exponential decay is insufficient measurement (or simulation) duration. Since we cannot observe ICT bigger than the measurement (or simulation) duration, the ICTD look like decaying exponentially at the tail. In this case, the ICTD still fits the truncated Pareto distribution since the original power law part of the ICTD is truncated by insufficient measurement duration as shown in Fig.7. Even though the ICTD is distorted by insufficient time, the routing delay distribution can be calculated by the same process introduced in the previous section. But there should be a difference in the delivery ratio since the measurement (or simulation) is ended before some messages reach their destinations.

Fig.7 shows an example of insufficient simulation time. The simulation has the same setup as in Figs.4 and 6. Both 600 hours and 300 hours of TLW make the same ICTDs, but for other cases the ICTD is truncated earlier and the delivery ratio is below one. From this figure, we can conclude that if the observed characteristic time is different from the analysis result by Eq.(11), the truncation is incurred by insufficient simulation duration. In this case, we can predict the delivery ratio is below one.

5. CONCLUSION

In this paper, we study the ICT patterns of human walks and routing performance in human driven DTNs. From the empirical ICT data analysis and its applications for routing performance analysis, we find the followings:

- The ICTD of human walks can be modeled by a truncated Pareto distribution. From this model, we can induce the closed form expression of the DTN routing delay distribution. While the existence of dichotomy in ICTD qualitatively suggest finite routing delays, we quantitatively show it.

- The TLW mobility model provides the same truncated Pareto ICTD as observed from the empirical data.

- The TLW mobility model enables us to quantify the characteristic time of human walks using the relaxation time theory. It can be used to predict the message delivery ratio.

We view that our work is an important step for the performance evaluation in human-driven DTN environments. Though there exist many studies on the patterns of ICTDs of human walks, they do not suggest quantitative approaches. Our work also points out that the ICTD patterns observed from measurement can be generated by TLW. Our work suggests a methodology both of analysis and simulation of human walks for the evaluation of DTN routing performance.

6. REFERENCES

[1] I. B. Aban, M. M. Meerschaert, and A. K. Panorska. Parameter estimation for the truncated pareto distribution. *Journal of the American Statistical Assoc.*, 101(473):270–277, March 2006.

[2] N. Agmon. Relaxation times in diffusion processes. *J. Chem. Phys.*, 82.

[3] J.-Y. L. Boudec and M. Vojnovic. The random trip model: Stability, stationary regime, and perfect simulation. *IEEE/ACM Trans. on Networking*, 14(6), December 2006.

[4] D. Brockmann, L. Hufnagel, and T. Geisel. The scaling laws of human travel. *Nature*, 439:462–465, January 2006.

[5] H. Cai and D. Y. Eun. Crossing over the bounded domain: From exponential to power-law inter-meeting time in manet. In *ACM Mobicom*, Montreal, Canada, 2007.

[6] T. Camp, J. Boleng, and V. Davies. A survey of mobility models for ad hoc network research. *Wireless Communications and Mobile Computing (WCMC): Special issue on Mobile Ad Hoc Networking: Research, Trends and Applications*, 2(5):482–502, March 2002.

[7] A. Chaintreau, P. Hui, J. Crowcroft, C. Diot, R. Gass, and J. Scott. Impact of human mobility on the design of opportunistic forwarding algorithms. In *Proc. of IEEE INFOCOM*, Barcelona, Spain, 2006.

[8] A. M. Edwards, R. A. Phillips, N. W. Watkins, M. P. Freeman, E. J. Murphy, V. Afanasyev, S. V. Buldyrev, M. G. E. da Luz, E. P. Raposo, H. E. Stanley, and G. M. Viswanathan. Revisiting levy flight search patterns of wandering albatrosses, bumblebees and deer. *Nature letters*, 449:1044–1048, 2007.

[9] K. Fall. A delay-tolerant network architecture for challenged internets. In *ACM Sigcomm*, 2003.

[10] M. Grossglauser and D. N. C. Tse. Mobility increases the capacity of ad hoc wireless networks. *IEEE/ACM Trans. on Networking*, 10(4):477–486, 2002.

[11] T. Henderson, D. Kotz, and I. Abyzov. The changing usage of a mature campus-wide wireless network. In *ACM Mobicom*, 2004.

[12] P. Hui, A. Chaintreau, J. Scott, R. Gass, J. Crowcroft, and C. Diot. Pocket switched networks and human mobility in conference environments. In *Proc. of ACM WDTN*, pages 244–251, Philadelphia, PA, 2005.

[13] A. Jindal and K. Psounis. Fundamental mobility properties for realistic performance analysis of intermittently connected mobile networks. In *Proceedings of the Fifth IEEE International Conference on Pervasive Computing and Communications Workshops*, 2007.

[14] J.Voit. *The Statistical Mechanics of Financial Markets*. Springer, 2005.

[15] T. Karagiannis, J.-Y. L. Boudec, and M. Vojnovic. Power law and exponential decay of inter contact times between mobile devices. In *ACM Mobicom*, Montreal, Canada, 2007.

[16] K.P.Burnham and D.R.Anderson. *Model Selection and Multimodel Inference, A practical Information Theoretic Approach, 2nd ed.* Springer, 2002.

[17] H. Lee. *Queueing Theory*. 1999.

[18] J. Leguay, A. Lindgren, J. Scott, T. Friedman, and J. Crowcroft. Opportunistic content distribution in an urban setting. In *Proc. of ACM SIGCOMM Workshops*, Pisa, Italy, 2006.

[19] M. McNett and G. M. Voelker. Access and mobility of wireless pda users. *SIGMOBILE Mob. Comput. Commun. Rev.*, 9(2):40–55, 2005.

[20] P.Bremaud. *Markov Chains, Gibbs Field, Monte Carlo Simulation and Queues*. Springer-Verlag, 1999.

[21] S. Redner. *A Guide to First-Passage Processes*. Cambridge University Press, 2001.

[22] I. Rhee, M. Shin, S. Hong, K. Lee, and S. Chong. On the levy walk nature of human mobility. In *IEEE INFOCOM*, 2008.

[23] R.N.Mantegna and H.E.Stanley. Stochastic Process with Ultraslow Convergence to a Gaussian: The Truncated Levy Flight. *Physical Review Letters*, 73, Nov. 1994.

[24] G. Sharma and R. R. Mazumdar. Scaling laws for capacity and delay in wireless ad hoc networks with random mobility. In *Proc. of IEEE ICC*, Paris, France, 2004.

[25] G. M. Viswanathan, S. V. Buldyrev, S. Havlin, M. G. E. da Luz, E. P. Raposo, and H. E. Stanley. Optimizing the success of random searches. *Nature*, 401:911–914, October 1999.